Structure-Based Design of (5-Arylamino-2*H*-pyrazol-3-yl)-biphenyl-2′,4′-diols as Novel and Potent Human CHK1 Inhibitors

Min Teng,*,† Jinjiang Zhu,† Michael D. Johnson,†
Ping Chen,‡ Jill Kornmann,§ Enhong Chen,§
Alessandra Blasina,§ James Register,‖ Kenna Anderes,§
Caroline Rogers,‡ Yali Deng,‡ Sacha Ninkovic,†
Stephan Grant,‖ Qiyue Hu,⊥ Karen Lundgren,§,#
Zhengwei Peng,⊥ and Robert S. Kania†

Department of Medicinal Chemistry, Biochemical Pharmacology, Research Pharmacology, Crystallography, and Computational Chemistry, Pfizer Global Research and Development, La Jolla, Inc., 10770 Science Center Drive, San Diego, California 92121-1194

Received April 18, 2007

Abstract: The cocrystal structure of a library hit was used to design a novel series of CHK1 inhibitors. The new series retained the critical hydrogen-bonding groups of the resorcinol moiety for binding but lacked the phenolic anilide moiety. The newly designed compounds exhibited similar enzymatic activity, while demonstrating increased cellular potency. Compound **10c**, showing no single agent effect, potentiated the antiproliferative effect of Gemcitabine in both prostate and breast cancer cell lines.

A eukaryotic cell cycle has a carefully regulated progression of phases: initial gap (G$_1$), DNA synthesis (S), secondary gap (G$_2$), and mitosis (M). Together, G$_1$, S, and G$_2$ are known as interphases. In G$_1$, the cell, whose biosynthetic pathways were slowed during mitosis, resumes a high rate of RNA and protein biosynthesis. The S phase begins when DNA synthesis starts and ends when the DNA content of the nucleus has been replicated. The cell then enters G$_2$, where RNA and protein biosynthesis occur once more. Following G$_2$, the cell enters M phase, which begins with nuclear division and ends with the complete division of the cytoplasm into two daughter cells. This marks the beginning of the interphase for new cells. Nondividing cells exist at G$_0$, a time following mitosis and before DNA synthesis.

Cells going into mitosis with damaged DNA will suffer from mitotic catastrophe, which ultimately leads to apoptosis. Therefore, in response to DNA damages, cells undergo various cell cycle arrests (G$_1$, S, G$_2$) to allow time for DNA repair.[1] Healthy cells have both G$_1$ and G$_2$ checkpoints.[2] The repair processes associated with G$_1$ and G$_2$ help to ensure cell viability after DNA damage by chemotherapy and radiation. Many types of cancer cells, however, rely exclusively on the G$_2$ checkpoint and its associated repair processes to remain viable and continue replication.[3] Abrogation of the G$_2$ checkpoint would leave cancer cells with no means to delay progression into mitosis following DNA damage.

Checkpoint enzymes, such as the serine/threonine protein kinase called checkpoint kinase 1 (CHK1[a1] or p56CHK1), are responsible for maintaining the order and fidelity of events in the cell cycle.[4] CHK1 plays an essential role in the regulation
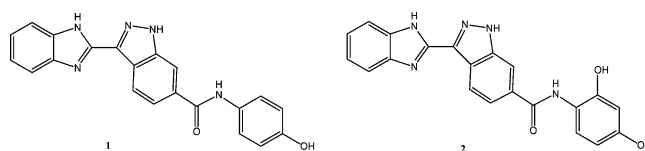
* To whom correspondence should be addressed. Tel.: (858) 401-8254. Fax: (858) 795-9333. E-mail: min.teng@biogenidec.com.
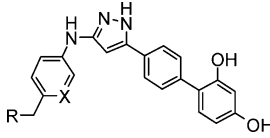† Department of Medicinal Chemistry.
‡ Department of Crystallography.
§ Department of Research Pharmacology.
‖ Department of Biochemical Pharmacology.
⊥ Department of Computational Chemistry.
Current address: 5200 Research Place, Biogen Idec, San Diego, CA 92122.

Figure 1. Our library hits: indazole CHK1 inhibitors.

of G$_2$ checkpoint by modulating Cdc25, a dual specificity phosphatase that activates Cdc2. In eukaryotes, Cdc2 is also known as cyclin-dependent kinase 1 (CDK1), which promotes mitotic entry.[5] CHK1 transduces signals from the DNA damage sensory complex to inhibit activation of Cdc2−cyclin B complex. CHK1 serves as the direct link between the G$_2$ checkpoint and the negative regulation of Cdc2. Inactivation of CHK1 has shown to abrogate G$_2$ arrest induced by DNA damage. When administered during the course of a DNA damaging event, such as chemotherapy employing antineoplastic agents, radiation therapy, immunotherapies, or antiangiogenic therapies, a CHK1 inhibitor should sensitize cancer cells, thereby triggering damage-mediated apoptosis. Meanwhile, healthy cells should retain G$_1$ checkpoint regulated by p53 to avoid death.[6] To not exacerbate the toxicities associated with chemo- and radiotherapies, an ideal CHK1 inhibitor should display no activity on its own. Administered as adjuvant therapeutics, a selective CHK1 inhibitor could prove beneficial for the treatment of cancer.[7]

There have been significant interests in the identification of CHK1 inhibitors.[8] Among the more well-known inhibitors is Staurosporine, a natural product whose analogs include an indolocarbazole (SB218078, SmithKline Beecham)[9] and 7-hydroxystaurosporine (UCN-01, NCI/Kyowa-Hakko),[10] the latter currently being evaluated in clinical trials as an anticancer agent.[11] These compounds display great inhibitory potency against both CHK1 and CDK1.[9] A number of other CHK1 inhibitors have been reported;[12] however, there is a clear need for potent and selective CHK1 inhibitors derived from a variety of chemotypes. Previously, our labs solved the structure of the human CHK1 kinase domain (residues 1−289) and its binary complex with AMP-PNP (1.7 Å), which facilitated the design of novel chemical classes.[13] Herein, we report the results of optimization of a screening hit using a structure-based drug design (SBDD) approach.

High-throughput screening of targeted libraries against the CHK1 kinase was employed to identify indazole CHK1 inhibitors represented by **1** and **2** (Figure 1). The library design was carried out by using an in-house tool called PGVL (Pfizer Global Virtual Library). Bearing an additional phenolic group, **2** showed significant improvement over **1** in terms of enzymatic potency against CHK1 (Table 1). When evaluated in the histone H3 ELISA assay, using camptothecin as the DNA damaging agent, **2** exhibited cellular activity of 550 nM, while **1** displayed no activity when tested at 1.0 uM and 10 uM.

To elucidate the enzymatic potency difference displayed by **1** and **2**, as well as to understand the binding mode of these indazoles, the X-ray cocrystal structures (1.7 Å) of **1** and **2** bound to the CHK1 enzyme were obtained. Both indazoles bind within the ATP binding pocket as anticipated (Figure 2a,b). For

Table 1. Biological Potency of Compounds **1**−**3**, **10a**−**g** at CHK1

cmpd	X	R	K_i^a (nM)	EC_{50}^b (nM)
1			301	NA^c
2			0.5	550
3			1.20	500
10a	CH	*iso*-propylamino	0.36	70
10b	CH	pyrrolidinyl	0.18	41
10c	CH	cyclopropylamino	0.38	60
10d	CH	dimethylamino	0.19	58
10e	N	piperidinyl	0.30	150
10f	N	*sec*-butylamino	0.20	230
10g	N	cyclopropylmethylamino	0.80	165

^{a} Data is the mean of duplicates with a SD of ±5%. ^{b} Data is the mean of duplicates with a SD of ±5.53%. ^{c} NA means no activity when tested at 1.0 uM and 10 uM.
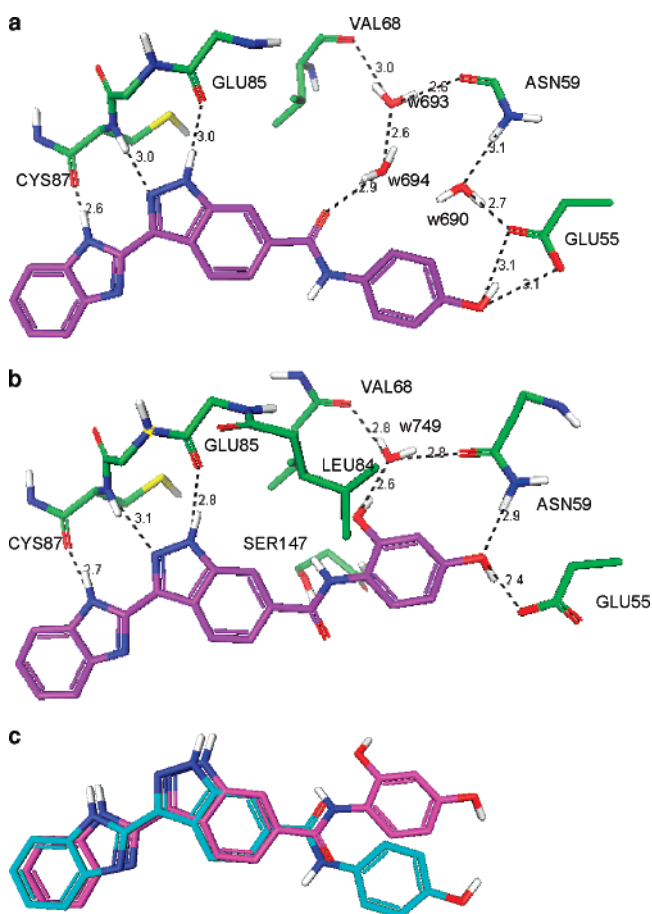

Figure 2. (a,b) Cocrystal structures of **1** and **2** bound to the ATP binding site of CHK1. To show H-bond interactions, hydrogen atoms are added for all cocrystal structures. (c) Overlay of X-ray structures of indazole **1** and **2** in the ATP binding pocket of CHK1.

Figure 3. Compounds **3** (aqua) and **2** (gold) as bound in the ATP binding site of CHK1.

as shown in Figure 2b. As a result, the phenolic anilide portion of the two inhibitors point in different directions (Figure 2c). This change of the amide conformation in **2** enables the 2-hydroxy to form an internal H-bond with the amide NH of **2** (2.30 Å) and a H-bond with w-749 (2.62 Å), which in turn forms H-bonds with Val68 (2.77 Å) and Asn59 (2.82 Å; Figure 2b). The 4-hydroxy group is in place to form a H-bond directly with Asn59 (2.93 Å), extruding w-690 in addition to forming a H-bond with Glu55 (2.43 Å). The sophisticated H-bond network involving w-749, Val68, Asn 59, Glu55, and the dihydroxy from the resorcinol moiety appears to be responsible for the superb potency of **2** against CHK1.

Although **2** showed excellent enzymatic potency against CHK1, its phenolic anilide feature was a concern due to the potential for it to form a reactive metabolite.[14] In addition, cellular potency required further improvement. Information gained from the cocrystal structures (Figure 2) indicated that, unlike **1**, the amide linker in **2** offered no interaction with the backbone of the CHK1 ATP pocket. The amide does, however, project the resorcinol head group to enable the desired hydrogen bond network. Moreover, in the environment where the amide linker resides there was additional unoccupied pocket space. A closer examination of this pocket revealed that it is lined mainly by lipophilic residues from Leu84 and Val68. This information inspired designs that replaced the amide linker in **2** with more liphophilic linkers that rigidly maintained proper distance and vectors to present the head group. These designs also targeted cellular potency optimization for which we aimed to improve permeability as a key strategy. In addition to amide replacement, we looked to reduce the desolvation penalty associated with the benzimidazole moiety. We replaced the benzimidazole with an amino pyridyl or amino phenyl group since these groups maintain the H-bond donating ability to the backbone carbonyl of Cys87 while possessing less polar surface areas.

The structural transformations used to accomplish these design principles evolved over time and are summarized as follows: First, the benzimidazole ring is changed into an aniline moiety as shown in **A** (Scheme 1). The next modification involves the truncation of the indazole ring into a pyrazole ring, as shown in **B**, preserving the acceptor−donor interactions with Cys87 and Glu85 of the enzyme. A new six-member ring is then constructed in the process of which the amide linker becomes an integral part of the ring, as in **C**. Conversion of the pyridone **C** into a phenyl ring leading to **3** completes the entire structural transformations. As a result, a phenyl ring in **3** is used as a rigid linker to replace the amide in **2**.

Compounds **3**, **10a**−**g** were synthesized according to previously described procedures.[15]

As expected, the cocrystal structure of **3** with the CHK1 enzyme (1.85 Å) was essentially identical to that of **2** with respect to the resorcinol region (Figure 3). This part of the molecule is clearly central to the binding of these inhibitors. The center phenyl ring now fills in the lipophilic "space" to create van der Waals interactions with the residue of Leu84.
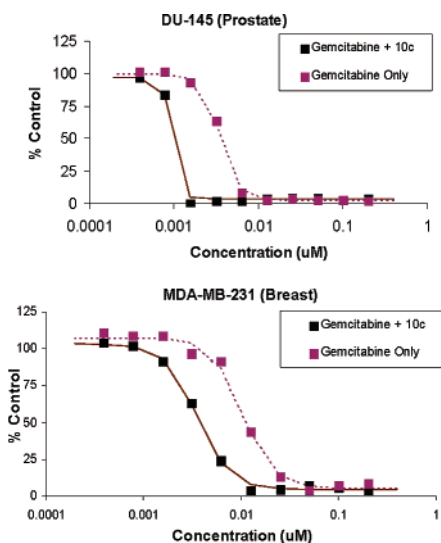
both compounds, the NH of the benzimidazole, together with the H-bound donor and acceptor of the indazole, form two H-bonds with Cys87 (backbone carbonyl and NH) and one with Glu85 (backbone carbonyl) of the hinge region of the CHK1 ATP binding pocket. Binding differences between **1** and **2** are derived from the differing anilide head groups. The *para*-hydroxy in **1** forms a H-bond with Glu55. The amide linker in **1** interacts with Val68 and Asn59 through w-694 and w-693 (Figure 2a). For **2**, the amide linker flips 180° to extrude w-694,
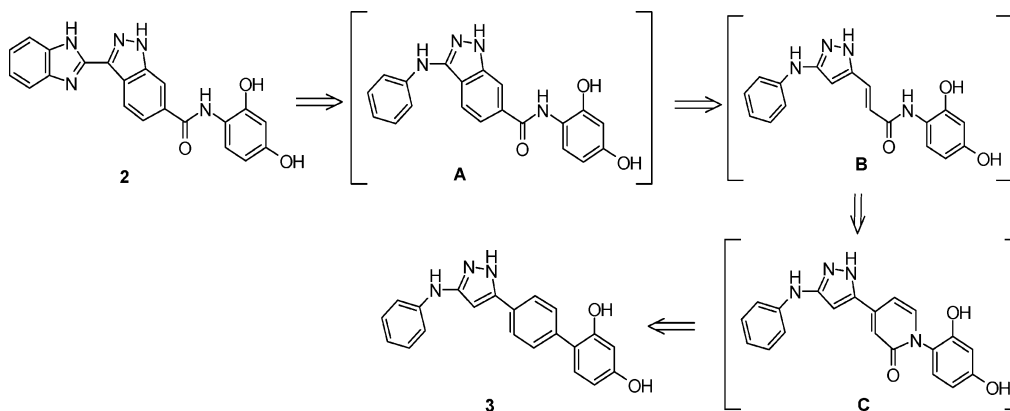
Scheme 1. Structural Transformation from Compound **2** to Compound **3** Guided by SBDD

Figure 4. Potentiation of the antiproliferative effect of Gemcitabine by **10c** at 0.24 uM.

The H-bond interactions between the pyazole nitrogens and Cys87 and Glu85 resemble that made by **2**. The NH from the aniline provides a hydrogen bond with Cys87. The *para*-position of the aniline is near the solvent channel with 5.5 Å from Glu91 and 3.9 Å from Asp94.

As seen in Table 1, **3** displayed enzymatic and cellular potency similar to that of **2** against CHK1. Clearly, the cell potency needed further improvement. As indicated above, further

structural modification at the *para*-position of the aniline could provide opportunities for further potency improvement. We decided to introduce an alkyl amino group to the *para*-position of the aniline or pyridyl ring. It was anticipated that this alkyl amino group would provide additional hydrogen bond interactions with Glu91 and Asp94 without significantly increasing the polar surface area of the molecule.

Table 1 lists a number of compounds with such a modification and their enzymatic and cellular potency against CHK1. As shown, the addition of a simple alkyl amino group to the *para*-position of the aniline or pyridyl amine improved both enzymatic and cellular activity compared to that of **3**. Compound **10a** was evaluated against a panel of 36 kinases. The selectivity data indicated that **10a** displayed good selectivity as its activity at CHK1 is at least 85-fold more potent than at other kinases.

Compound **10c** was evaluated for the potentiation of the growth inhibitory activity of Gemcitabine in prostate and breast cancer cell lines in the MTT assay. In this assay, increasing concentrations of Gemcitabine were used in combination with 240 nM of **10c**. When used alone, **10c** induced no or minimal cellular toxicity (Figure 4). The combination treatment resulted in greater activity (IC$_{50}$ of 1.0 nM in prostate, 3.8 nM in breast cancer cells) than the treatment by Gemcitabine alone (IC$_{50}$ of 3.5 nM in prostate, 11.4 nM in breast cancer cells). These results provided evidence for the in vitro efficacy of **10c** in enhancing the cancer cell killing activity of Gemcitabine with minimal single agent activity attributed to **10c** alone.

To demonstrate that the synergy with Gemcitabine is due to the inhibition of CHK1 through the abrogation of the S
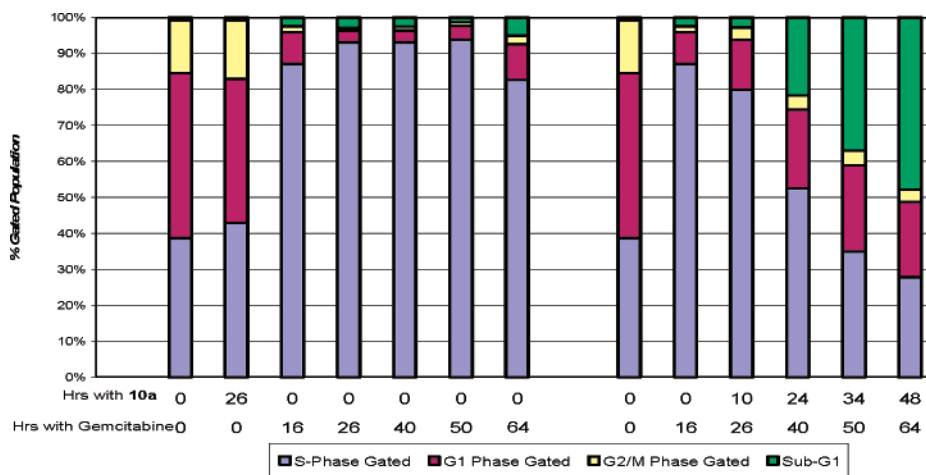

Figure 5. Fluorescence activated cell sorting (FACS) results of **10a** in combination with Gemcitabine.

checkpoint, fluorescence activated cell sorting (FACS) was performed with **10a** in MDA-MB-231 cell line. As shown in Figure 5, **10a** alone (560 nM) displayed an insignificant effect on cell cycle, while Gemcitabine alone (10 nM) induced a prominent S phase arrest at 16 h post-treatment. In the combination treatment, flow cytometry analysis showed abrogation of Gemcitabine-induced S phase arrest. The time-dependent decrease in the S phase cells induced by **10a** corresponded to an increase in the G_2-M and G_0-G_1 cell populations, indicating that the cells were entering mitosis and attempting to re-enter the cell cycle. In addition, an increase in the population of sub-G_1 cells was detected in the combination-treated cells, indicating apoptotic cell death.

In conclusion, we have identified novel and potent CHK1 inhibitors through structural transformations of a library hit using SBDD. Through these exercises, we have illustrated how the structural information about the target guided us to formulate and test our ideas. Using this powerful tool, we have removed the phenolic anilide feature from the original hit and improved cellular potency. Compound **10c** potentiated the growth inhibitory activity of Gemcitabine in both prostate and breast cancer cell lines. Broader SAR and other biological attributes regarding the newly identified pyrazole inhibitors will be subjects of future investigations to be reported in due course.

Note Added after ASAP Publication. This manuscript was released ASAP on September 21, 2007 before final corrections were incorporated. The corrected version was posted on September 27, 2007.

Supporting Information Available: Synthesis procedures and characterization data for intermediates and final compounds. Procedures for enzymatic, cellular, MTT, and FACS assays. Crystallization conditions and X-ray data statistics for **1**, **2**, and **3**. Kinase selectivity profile for **10a**. This material is available free of charge via the Internet at http://pubs.acs.org.

References

(1) Zhou, B.-B.; Elledge, S. J. The DNA Damage Response: Putting Checkpoints in Perspective. *Nature* **2000**, *408*, 433–439. (b) Melo, J.; Toczyski, D. A Unified View of the DNA-Damage Checkpoint. *Curr. Opin. Cell Biol.* **2002**, *14*, 237–245.

(2) Li, Q.; Zhu, G.-D. Targeting Serine/Threonine Protein Kinase B/Akt and Cell-Cyclo Checkpoint Kinases for Treating Cancer. *Curr. Top. Med. Chem.* **2002**, *2*, 939–971.

(3) Kastan, M. B.; Onyekwere, O.; Sidransky, D.; Vogelstein, B.; Craig, R. W. Participation of p53 Protein in the Cellular Response to DNA Damage. *Cancer Res.* **1991**, *51*, 6304–6311. (b) Greenblatt, M. S.; Bennett, W. P.; Hollstein, M.; Harris, C. C. Mutations in the p53 Tumor Suppressor Gene: Clues to Cancer Etiology and Molecular Pathogenesis. *Cancer Res.* **1994**, *54*, 4855–4878..

(4) Sancar, A.; Lindsey-Boltz, L. A.; Unsal-Kacmaz, K.; Linn, S. Molecular Mechanisms of Mammalian DNA Repair and the DNA Damage Checkpoints. *Annu. Rev. Biochem.* **2004**, *73*, 39–85. (b) Nasmyth, K. Putting the Cell Cycle in Order. *Science* **1996**, *274*, 1643.

(5) Peng, C.-Y.; Graves, P. R.; Thoma, R. S.; Wu, Z.; Shaw, A. S.; Piwnica-Worms, H. Mitotic and G2 Checkpoint Control: Regulation of 14-3-3 Protein Binding by Phosphorylation of Cdc25C on Serine-216. *Science* **1997**, *277*, 1501–1505. (b) Furnari, B.; Rhind, N.; Russell, P. Cdc25 Mitotic Inducer Targeted by Chk1 DNA Damage Checkpoint Kinase. *Science* **1997**, *277*, 1495–1497.

(6) Nurse, P. Checkpoint Pathways Come of Age. *Cell* **1997**, *91*, 865–867. (b) Weinert, T. Cell Cycle: A DNA Damage Checkpoint Meets the Cell Cycle Engine. *Science* **1997**, *277*, 1450–1451. (c) Walworth, N.; Davey, S.; Beach, D. Fission Yeast *chkl* Protein Kinase Links the *rad* Checkpoint Pathway to *cdc2*. *Nature* **1993**, *363*, 368–371.

(7) Certain CHK-1 inhibitors have been proposed for cancer therapy. (a) Sanchez, Y.; et al. Conservation of the Chk1 Checkpoint Pathway in Mammals: Linkage of DNA Damage to Cdk Regulation through Cdc25. *Science* **1997**, *277*, 1497–1501. (b) Flaggs, G.; et al. Atm-Dependent Interactions of a Mammalian Chk1 Homolog with Meiotic Chromosomes. *Curr. Biol.* **1997**, *7*, 977–986.

(8) Prudhomme, M. Novel Checkpoint 1 Inhibitors. *Rec. Pat. Anti-Cancer Drug Discovery* **2006**, *1*, 55–68. (b) Tao, Z.-F.; Lin, N.-H. Chk1 Inhibitors for Novel Cancer Treatment. *Anti-Cancer Agents Med. Chem.* **2006**, *6*, 377–388.

(9) Jackson, J. R.; Gilmartin, A.; Imburgia, C.; Winkler, J. D.; Marshall, L. A.; Roshak, A. An Indolocarbazole Inhibitor of Human Checkpoint Kinase (Chk1) Abrogates Cell Cycle Arrest Caused by DNA Damage. *Cancer Res.* **2000**, *60*, 566–572.

(10) Graves, P. R.; Yu, L.; Schwarz, J. K.; Gales, J.; Sausville, E. A.; et al. The CHK1 protein Kinase and the Cdc25C Regulatory Pathways are Targets of the Anticancer Agent UCN-01. *J. Biol. Chem.* **2000**, *275*, 5600–5605. (b) Busby, E. C.; Leistritz, D. F.; Abraham, R. T.; Karnitz, L. M.; Sarkaria, J. N. The Radiosensitizing Agent 7-Hydroxystaurosporine (UCN-01) Inhibits the DNA Damage Checkpoint Kinase hCHK1. *Cancer Res.* **2000**, *2000*, 2108–2112.

(11) Sausville, E. A.; Arbuck, S. G.; Messmann, R.; Headless, D.; Lush, R. D.; et al. Phase I Trial of 72-Hour Continuous Infusion UCN-01 in Patients with Refractory Neoplasms. *J. Clin. Oncol.* **2001**, *19*, 2319–2333. (b) Senderowicz, A. M. The Cell Cycle as a Target for Cancer Therapy: Basic and Clinical Findings with the Small Molecule Inhibitors Flavopirodol and UCN-01. *Oncologist* **2002**, *7*, 12–19.

(12) Foloppe, N.; Fisher, L. M.; Francis, G.; Howes, R.; Kierstan, P.; Potter, A. Identification of a Buried Pocket for Potent and Selective Inhibition of CHK1: Prediction and Verification. *Bioorg. Med. Chem.* **2006**, *14*, 1792–1804 and references cited therein. (b) Tao, Z.-F.; et al. Structure-Based Design, Synthesis, and Biological Evaluation of Potent and Selective Macrocyclic Checkpoint Kinase 1 Inhibitors. *J. Med. Chem.* **2007**, *50* (7), 1514–1527. (c) Tong, Y.; et al. Discovery of 1,4-Dihydroindeno[1,2-*c*]pyrazoles as a Novel Class of Potent and Selective Checkpoint Kinase 1 Inhibitors. *Bioorg. Med. Chem.* **2007**, *15*, 2759–2767.

(13) Chen, P.; Luo, C.; Deng, Y.; Ryan, K.; Register, J.; Margosiak, S. Tempczyk-Russell, A.; Nguyen, B.; Myers, P.; Lundgren, K.; Kan, C.-C.; O'Connor, P. M. The 1.7 Å Crystal Structure of Human Cell Cycle Checkpoint Kinase Chk1: Implications for Chk1 Regulation. *Cell* **2000**, *100*, 681–692.

(14) Benya, T. J.; Cornish, H. H. Toxicology of Aromatic Nitro and Amino Compounds. Patty's Industrial Hygiene and Toxicology (4th Edition). **1994**, *2* (Pt. B), 947–1085. (b) Kazius, J.; McGuire, R.; Bursi, R. Derivation and Validation of Toxicophores for Mutagenicity Prediction. *J. Med. Chem.* **2005**, *48* (1), 312.

(15) Johnson, M. D.; Teng, M.; Zhu, J. Preparation of aminopyrazoles as CHK1 checkpoint protein kinase inhibitors. U.S. patent application, WO 2005009435, 2005.